ANALES DE LA REAL ACADEMIA NACIONAL DE FARMACIA
ISSN (Online) 1697-4298
Article
analesranf.com

Targeting inflammation in the retina: a new therapeutic approach in diabetic retinopathy

Title in Spanish: *El tratamiento de la inflamacion en la retina: una nueva estrategia terapéutica en la retinopatía diabética*

Ana I. Arroba[1,2*], Ángela M. Valverde[1,2]

[1]Alberto Sols Biomedical Research Institute (IIBm) (CSIC/UAM), 28029 Madrid, Spain. [2]Spanish Biomedical Research Centre in Diabetes and Associated Metabolic Disorders (CIBERdem), ISCIII, 28029 Madrid, Spain.

ABSTRACT: Retinal diseases linked to inflammation, including diabetic retinopathy (DR), are often accompanied by resident macrophage/microglial cells activation. During DR, there are substantial changes in the polarization status of the microglia from the M2 (anti-inflammatory) to the M1 (pro-inflammatory) stage. However, the dynamics between M1 and M2 polarization of microglia during DR has not been investigated and it might be therapeutically useful. In this study, we have characterized the evolution of microglia polarizarion during the early stages of DR in the retina of diabetic *db/db* mice. Moreover, we have analyzed microglia polarization in response to pro-(bacterial lipopolysaccharide; LPS) or anti-(IL4/IL13 cytokines or the bicyclic nojirimycin derivative (1*R*)-1-dodecylsulfinyl-5*N*,6*O*-oxomethylidenenojirimycin (*R*-DS-ONJ)) inflammatory stimuli. For this goal, we have performed in vitro experiments in Bv-2 murine microglial cells as well as ex vivo experiments in retinal explants from *db/db* mice. Treatment of Bv-2 cells with LPS together with IL4/IL13 or *R*-DS-ONJ switched the M1 response towards M2. In retinal explants from *db/db* mice, *R*-DS-ONJ induced a M2 response. In conclusion, the modulation of microglia polarization dynamics towards a M2 status at early stages of DR offers novel therapeutic interventions.

RESUMEN: Las enfermedades retinianas, entre las que se encuentra la retinopatía diabética (RD), están vinculadas a un contexto inflamatorio en el cual existe una activación de los macrófagos residentes en la retina (microglia). Durante la retinopatía diabética se producen cambios de polarización de la microglia, definiéndose éstos como transiciones entre el estado M1 (pro-inflamatorio) y el estado M2 (anti-inflamatorio), estando aún por determinar los tiempos de aparición y actuación de la microglia en cada uno de ellos. La identificación espacio-temporal de la transición de la microglía de un estado a otro podría constituir una potente herramienta clínica para diferentes abordajes terapéuticos. En este trabajo se ha caracterizado el estado de polarización de la microgía en la retina durante las primeras fases de la RD en el modelo de ratón diabético *db/db*. Además, se ha estudiado la polarización de la microglia en presencia de estímulos pro-inflamatorios (lipopolisacárido bacteriano; LPS) o anti-inflamatorios (citoquinas IL4/IL13 o un compuesto natural derivado de la casternospermina, R-DS-ONJ). Para ello, se ha realizado un abordaje in vitro utilizando la línea celular de microglia murina Bv-2 y un abordaje ex vivo con explantes de retinas procedentes de ratones diabéticos *db/db*. El tratamiento de las células Bv-2 con LPS en combinación con IL4/IL13 o alternativamente con el compuesto R-DS-ONJ indujo la transición en la polarización de la microglia desde el estado pro-inflamatorio M1, inducido por el LPS, al estado anti-inflamatorio M2. En los explantes de retinas de ratones *db/db*, el compuesto R-DS-ONJ indujo la respuesta M2 disminuyendo la respuesta M1. En conclusión, la polarización de la microglia hacía un estado M2 durante los estadíos tempranos de la RD ofrece una nueva ventana terapéutica de actuación.

[*]**Corresponding Author:** aarroba@iib.uam.es
An Real Acad Farm Vol. 83, Nº 1 (2017), pp. 81-92
Received: Mars 21, 2017 **Accepted:** Mars 22, 2017
Language of Manuscript: English
Premio del Consejo General de Colegios Oficiales Farmacéuticos del Concurso científico 2016 de la Real Academia Nacional de Farmacia

1. INTRODUCTION

Insulin resistance and chronic inflammation are implicated in the pathogenesis of type 2 diabetes (T2D) and in diabetic retinopathy (DR), its most prevalent

complication (1). In fact, neuroinflammation induced by the diabetic milieu is a central contributing factor in DR progression (2). Similarly to other neurodegenerative diseases, DR exhibits characteristics of low-grade chronic inflammation (3) in which changes in retinal expression of inflammatory mediators occur in concert with functional changes in retinal permeability and apoptosis (4, 5). It has been proposed that in neuroinflammation microglia becomes activated and produce inflammatory mediators. Microglia, serving as resident macrophages of the retina, has multiple functional states and carries out diverse functions. Capable of rapid dynamism and motility, microglial cells synthesize and release cytokines, chemokines, neurotrophic factors, and neurotransmitters that interact with multiple cell types in the central nervous system (CNS) and exert cytotoxic, cytoprotective and scavenger effects depending on the tissue context (6). Retinal diseases such as proliferative DR and diabetic macular edema are often accompanied by macrophage/microglia cells activation (7, 8).

The existence of a continuum of polarization states in macrophages results from the integration of the intracellular signals triggered by their surrounding milieu (9, 10). M1, or classically-activated macrophages, mainly secrete pro-inflammatory cytokines such as TNFα, IL12, IL23, IL1β, IL6 and chemotactic factors and are involved in the pro-inflammatory response. By contrast, alternatively-activated macrophages (M2) express high levels of arginase-1 and IL10, but low levels of IL12 and IL23 and are usually induced by the anti-inflammatory cytokines IL4 and IL13 (11).

DR exhibits many features of chronic inflammation such as increased NO production and release of pro-inflammatory cytokines (12). In fact, TNFα, IL1β, IL-8 and MCP-1 have been found elevated in the vitreous of diabetic patients (13, 14). Recently, the inflammasome complex, which cleaves pro-IL1β into secreted IL1β via caspase-1, has been found activated in retinal pigment epithelial cells cultured under high glucose levels (15), but its modulation in the retina during DR has not yet been explored. In this scenario, microglia may underline its different functional properties and, therefore, targeting its polarization is a promising approach for the treatment of CNS diseases (16) including DR.

Among therapies targeting pro-inflammatory mediators, the natural compounds have emerged as an alternative to chemical drugs. Iminosugar glycosyl hydrolase inhibitors such as 1-deoxynojirimycin and castanospermine have a strong potential in therapies for cancer, viral infections, diabetes and glycosphingolipid storage disorders (17, 18). In particular, sp^2-iminosugar-type bicyclic nojirimycin analogues with an alpha-configured *N*-, *S*-, or *C*-linked pseudoanomeric group have been previously evaluated as antitumor agents (18). However, their effects in inflammatory processes during DR remain to be elucidated.

In recent years the C57BL/KsJ-*db/db* mouse model has been extensively used to investigate the pathogenesis of DR (19) since reproduce the neurodegenerative process that occur in the human diabetic retina (20). However, the events that occur in the retina at early stages of DR previous to neurodegeneration, and, in particular the role of microglia associated to neuroinflammation in *db/db* mice remain unknown. The aim of this study is to examine the polarization of microglia during the early stages of DR and its modulation by a sp^2-iminosugar-type bicyclic nojirimycin analogue.

2. METHODS

2.1. Reagents and drugs

Fetal bovine serum (FBS) and culture media were obtained from Invitrogen (Grand Island, NY, USA). Bovine serum albumin (BSA) and bacterial lipopolysaccharide (LPS) were purchased from Sigma-Aldrich (St Louis, MO, USA). IL4 and IL13 were purchased from Preprotech (London, UK). Bradford reagent, acrylamide, immunoblot PVDF membranes and chemioluminiscent HRP Substrate were purchased from Bio-Rad (Madrid, Spain).

2.2. Cell culture

Mouse microglia Bv-2 cell line was provided by Dr. M.L. Nieto (CSIC, Spain). Bv-2 cells were cultured at 37°C in a humidified atmosphere with 5 % CO_2 in RPMI supplemented with 10 % (v/v) heat-inactivated FBS, 1 % (v/v) penicillin/streptomycin (Sigma) and 2 mM L-glutamine (Gibco, Carlsbad, California, USA). Cells were grown up to 70 % confluence, washed with PBS and further stimulated in serum-free medium with LPS (200 ng/ml) with or without a mixture of IL4/IL13 (20 ng/ml each; M2) or R-DS-ONJ (compound C5) for several time-periods. For mouse cell line authentication, genomic DNA was isolated from Bv-2 cells and analyzed by PCR as described (21). Primer sequences used for amplification of mouse STR were: Forward (6-7) 5′AGTCCACCCAGTGCATTCTC 3′; Reverse (6-7) 5′CATGTGGCTGGTATGCTGTT 3′; Forward (15-3) 5′ TCTGGGCGTGTCTGTCATAA 3′: Reverse (15-3) 5′ TTCTCAGGGAGGAGTGTGCT 3′.

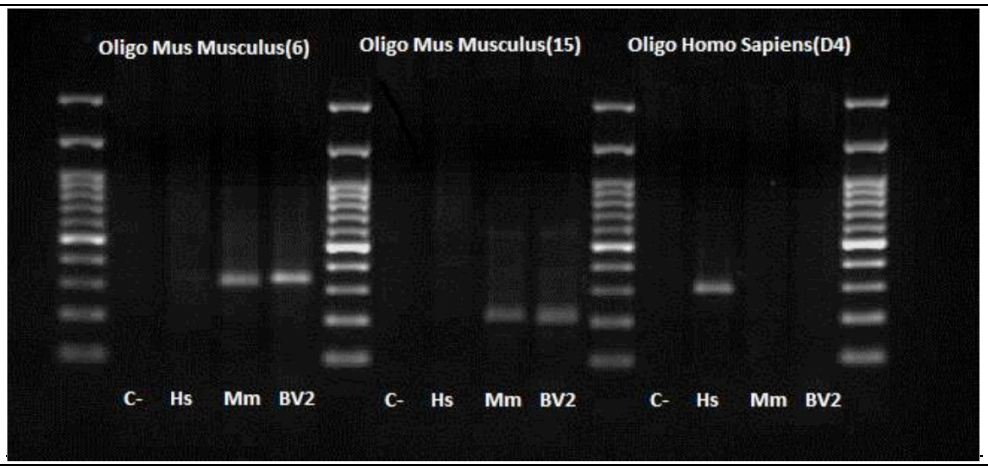

Figure 1. Murine Cell line authentication. Bv.2 murine microglia cell line was authenticated at IIBM Genomic Core Facility. HS: *Homo sapiens* control DNA; Mm: *Mus musculus* control DNA.

2.3. Animals and retina isolation

C57BL/KsJ *db/db* and *db/+* male mice were purchased from Harlan (Harlan Laboratories, Inc. UK). Mice were maintained in light/dark (12-hours light/12-hours dark)-, temperature (22°C)- and humidity-controlled rooms, and fed ad libitum with free access to water. All animal experimentation followed recommendations of the Federation of European Laboratory Animal Science Associations (FELASA) on health monitoring in accordance with the regulations of the Association for Research in Vision and Ophthalmology. Animals were killed by cervical dislocation and eyes were enucleated. The lens, anterior segment, vitreous body, retinal pigment epithelium and sclera were removed.

2.4. Retinal explants

Ex vivo assays were performed with retinas from 8 weeks old male *db/+* and *db/db* mice as previously described (22). Following isolation, retinas were cultured in R16 medium (provided by Dr. P.A. Ekstrom, Lund University, Sweden) with no additional serum. Retinas were stimulated with *R*-DS-ONJ (compound C5) at 50 µM for 24 h as indicated in the figure legends.

2.5. Analysis of cellular viability

Bv-2 cells were seeded in 24-well plates and allowed to stabilize overnight. The cells were then treated with *R*-DS-ONJ (1-50 µM) for 24 h. Following incubation, the viability of the cells was measured with crystal violet as described (23).

2.6. Analysis of Nitrites (NO_2^-)

Levels of NO_2^- were measured using the Griess method (24). In an acidic solution with 1 % sulphanilamide and 0.1 % N-(1-Naphthyl) ethylenediamine (NEDA), nitrites convert into a pink compound that is colorimetric calculated at 540 nm in a microplate reader (Versamax Tunable Microplate reader, Molecular Devices, Sunnyvaley, CA, EEUU).

2.7. Western blot

Whole retinas or Bv-2 cells were homogenized in lysis buffer containing 50 mM Tris-HCl, 1 % Triton X-100, 2 mM EGTA, 10 mM EDTA acid, 100 mM NaF, 1 mM $Na_4P_2O_7$, 2 mM Na_3VO_4, 100 µg/mL phenylmethylsulphonyl fluoride, 1 µg/mL aprotinin, and 1 µg/mL leupeptin, supplemented with protease inhibitors (10 µg/ml leupeptin, 10 µg/ml aprotinin, and 100 µg/ml phenylmethylsulphonyl fluoride). All debris was removed by centrifugation at 14,000 x g for 10 min at 4ºC and protein concentration was quantified using the Bio-Rad protein assay with BSA as a standard. Equivalent amounts of protein were resolved using denaturing sodium dodecyl sulphate-polyacrilamide gel electrophoresis (SDS-PAGE), followed by transfer to PVDF membranes (Bio-Rad). Membranes were blocked using 5 % non-fat dried milk or 3 % BSA in 10 mM Tris-HCl, 150 mM NaCl, pH 7.5 (TBS), and incubated overnight with several antibodies (1:2000 unless otherwise stated) in 0.05 % Tween-20-TBS. Immunoreactive bands were visualized using the enhanced chemioluminiscence reagent (Bio-Rad). Antibodies against iNOS (sc- 650), IκBα (sc-371), NFkB p65(C-20) (sc-372), JNK (sc-571), phospho-38 MAPK (Thr180/Tyr182) (sc-17852-R) and p38 MAPK (sc-9212) were purchased from Santa Cruz Biotechnology (Palo Alto, CA, USA). Anti-phospho-JNK (Thr183/Tyr185) (#4668) antibody was purchased from Cell Signaling Technology (MA, USA). Anti-Arginase-1 (BD 610708) was purchased from BD Biosciences (Madrid, Spain). Anti-α-tubulin (T-5168) antibody was from Sigma Chemical Co. (St Louis, MO, USA).

2.8. Immunofluorescence

Eyes, retinal explants or Bv-2 cells were fixed in 4 % paraformaldehyde for 24 h at 4°C and infiltrated with sucrose 25 % (w/v). For immunofluorescence analysis, we followed the protocol previously detailed (25). The samples were then incubated overnight in a humid chamber at 4 ºC with rabbit anti-GFAP (glial fibrillary acidic protein) (1:1000), mouse anti-arginase-1 (1:1000) and rabbit anti-iNOS (1:1000) antibodies in blocking solution. Samples were washed and incubated for 90 min with anti-rabbit, anti-mouse, anti-goat or anti-rat

immunoglobulin antibodies conjugated to Alexa 647 or 488 (1:2000; Molecular Probes, Eugene, OR). After washing, sections were mounted with medium (Fluoromount G) containing 4-6-diamidino-2-phenylindole (DAPI). Staining was observed with an inverted laser confocal microscope LSM710 (Carl Zeiss Microscopy GmbH, Göttingen, Germany).After washing, sections were mounted with medium (Fluoromount G) containing 4-6-diamidino-2-phenylindole (DAPI). Staining was observed with an inverted laser confocal microscope LSM710 (Carl Zeiss Microscopy GmbH, Göttingen, Germany).

2.9. Endotoxin detection

Serum endotoxin concentrations were measured with a commercial kit (QAYEE-BIO; Deltaclon, Madrid, Spain) according to the manufacturer's instructions. Briefly, blood samples were collected in non-pyrogenic and endotoxin-free tubes, centrifuged at 2,500 x g for 10 min and serum was separated. Samples were diluted (1/5) with endotoxin-free water and horseradish peroxidase (HRP) was added. Samples were gently shacked, incubated for 60 min at 37°C and then washed 5 times. Chromogen solution A was added to the samples that were gently shacked and further incubated for 10 min at 37ºC protected from light. Finally, stop solution was added and samples were measured at 450 nm.

2.10. Quantitative real-time PCR (qRT-PCR)

Total RNA was extracted with Trizol® reagent (Invitrogen, Madrid, Spain) and reverse transcribed using a SuperScript™ III First-Strand Synthesis System for RT-qPCR following the manufacturer's indications (Invitrogen). RT-qPCR was performed with an ABI 7900 sequence detector. Primer-probe sets for mouse TNFα, IL6, IL1β, iNOS, arginase-1 and 18s were purchased as predesigned TaqMan gene expression assays (Applied Biosystems, Spain).

2.11. Statistical analysis

Densitometry of the Western blots was performed using the Image J program. Values in all graphs represented the mean ± SEM. Statistical tests were performed using SPSS 21.0 for Windows (SPSS Inc. IBM, Armonk, NY, USA). Data were analyzed by one-way ANOVA followed by Bonferroni t-test or by paired t-test when comparisons were among two groups. Differences were considered significant at *p≤ 0.05.

3. RESULTS

3.1. LPS-treated Bv-2 cells induced a pro-inflammatory response that was reduced by co-treatment with M2 cytokines or the sp^2-iminosugar derivative R-DS-ONJ

We stimulated Bv-2 cells, a mouse microglia cell line, with LPS (M1 stimulus) in the absence or presence of M2 cytokines (IL4/IL13). LPS was used as a pro-inflammatory stimulus since it induces an environment similar to that found in the obesity-related diabetic context (26). Based on that, Bv-2 cells were cultured in the presence of LPS, IL4/IL13 (M2) and the combination of both (LPS+M2). Figure 2A shows that the release of nitrites in the culture medium in LPS-treated Bv-2 cells was significantly reduced by the co-treatment with IL4/IL13. Likewise, iNOS, which was elevated in LPS-treated Bv-2 cells, significantly decreased by the co-treatment with M2 cytokines (Figure 2B). Conversely, arginase-1 decreased by LPS treatment, this effect being ameliorated in the combination of LPS plus IL4/IL13. The effect of M2 cytokines was also evident by the decrease of LPS-induced mRNA levels of TNFα, IL1β, IL6 and iNOS (Figure 2C).

We tested a pharmacological approach using the sp^2-iminosugar dodecylsulfoxide derivative *R-DS-ONJ* (referred as C5; Figure 3A). As shown in Figure 3B, the viability of Bv-2 cells exposed to *R-DS-ONJ* (50 μM) was not affected. In Bv-2 cells cultured with LPS plus *R-DS-ONJ*, nitrite production and iNOS expression (mRNA and protein) were reduced as compared to the LPS condition (Figure 3C, 3D, 3E). *R-DS-ONJ* also decreased mRNA levels of the pro-inflammatory cytokines IL1β and IL6 (Figure 3E).

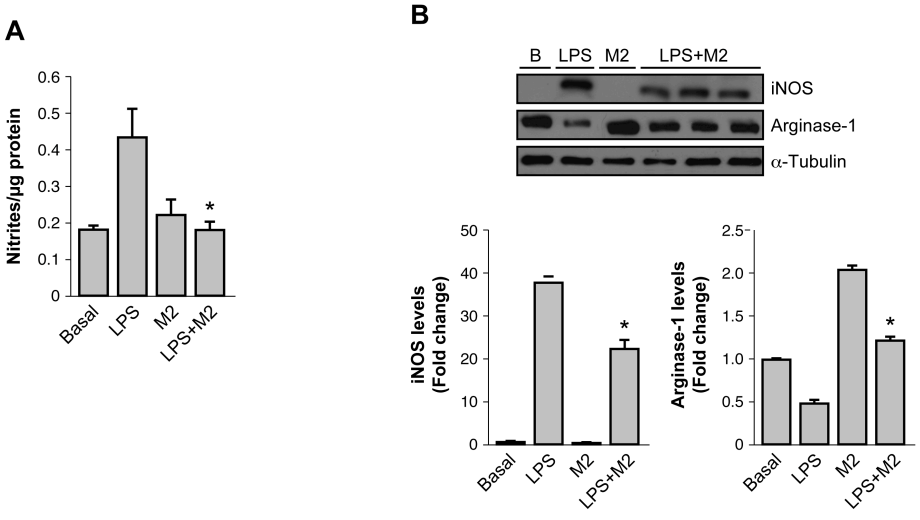

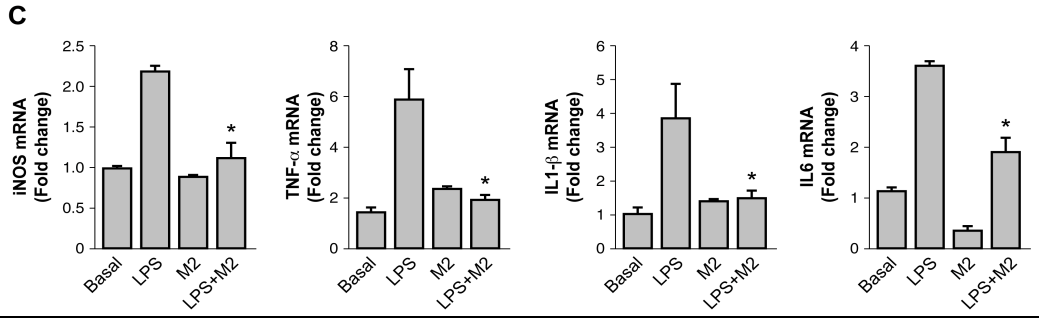

Figure 2. IL4/IL13 (M2 cytokines) prevented the pro-inflammatory effects of LPS in Bv-2 microglia cells. Bv-2 cells were treated with LPS (200 ng/ml) in the absence or presence of IL4/IL13 (20 ng/ml each). A) Nitrites in the culture medium. B) Western blot for arginase-1 and iNOS. C) mRNA levels of TNFα, IL1β, IL6 and iNOS. Results are expressed as $2^{-\Delta Ct}$. Results are means ± SEM (n=5 independent experiments); *p≤0.05 LPS+M2 *vs* LPS.

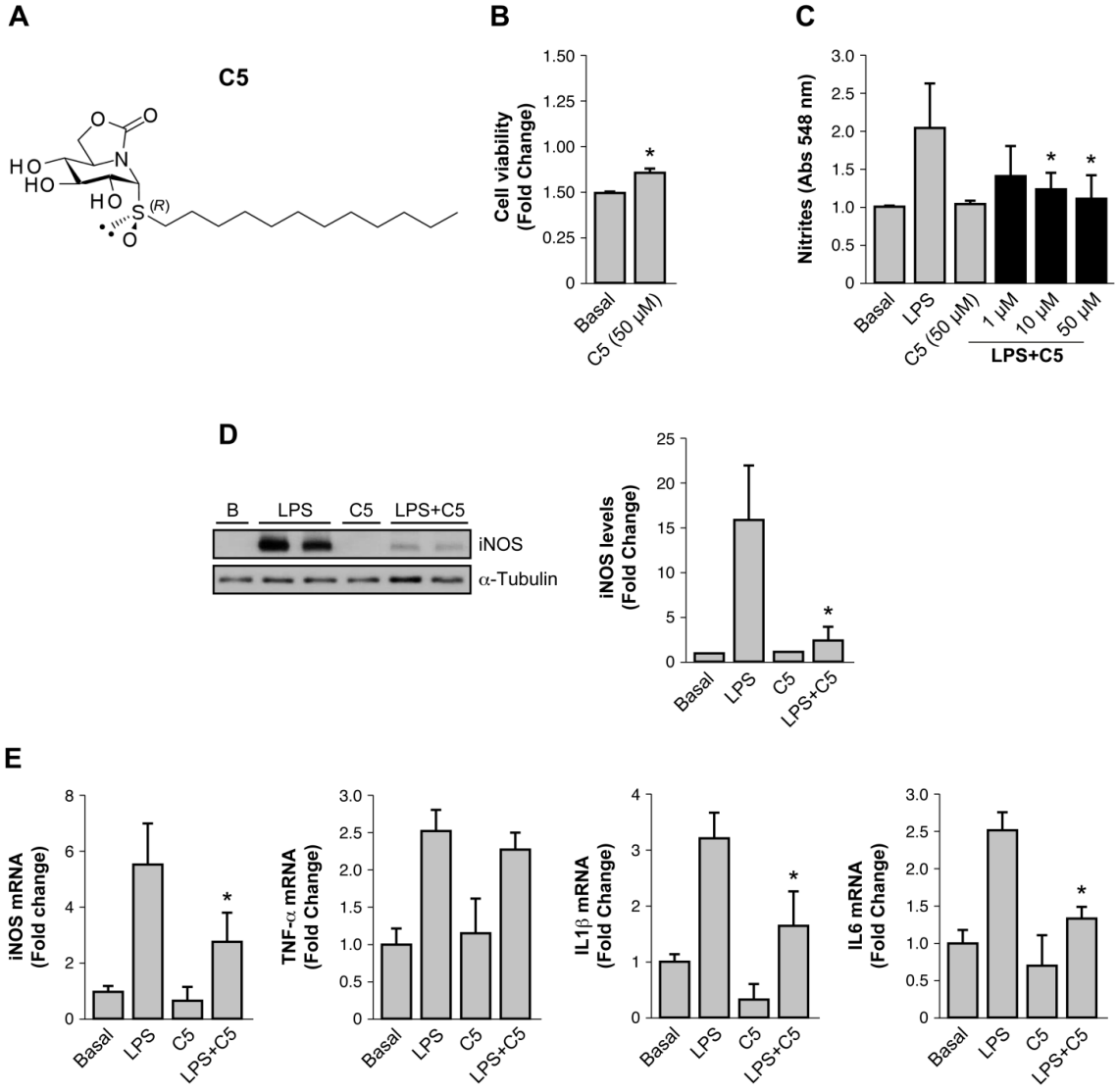

Figure 3. Sp^2-iminosugar dodecylsulfoxide *R*-DS-ONJ (compound 5) prevented LPS-mediated effects in Bv-2 microglia cells and increased arginase-1 in retinal explants. Bv-2 cells were treated with LPS (200 ng/ml) in the absence or presence of (1*R*)-1-dodecylsulfinyl-5*N*,6*O*-oxomethylidenenojirimycin (*R*-DS-ONJ, referred as C5 in the figures) at the indicated doses. A) Chemical structure of C5 compound. B) Crystal violet staining. C) Nitrites accumulation. D) Western blot for iNOS using α-Tubulin as a loading control. E) mRNA levels of TNFα, IL1β, IL6 and iNOS. Results are expressed as $2^{-\Delta Ct}$. Results are means ± SEM (n=5 independent experiments); *p≤0.05 LPS+*R*-DS-ONJ *vs* LPS.

3.2. M2 cytokines or sp²-iminosugar derivative R-DS-ONJ decreased the pro-inflammatory signaling pathways induced by LPS in Bv-2 cells

We also evaluated the impact of M2 cytokines or *R-DS-ONJ* in the early pro-inflammatory signaling pathways activated by LPS in Bv-2 cells. As Figure 4 shows, co-treatment with M2 cytokines prevented LPS-mediated IκBα degradation, the phosphorylation of JNK, but this effect was less evident in the phosphorylation of p38 MAPK.

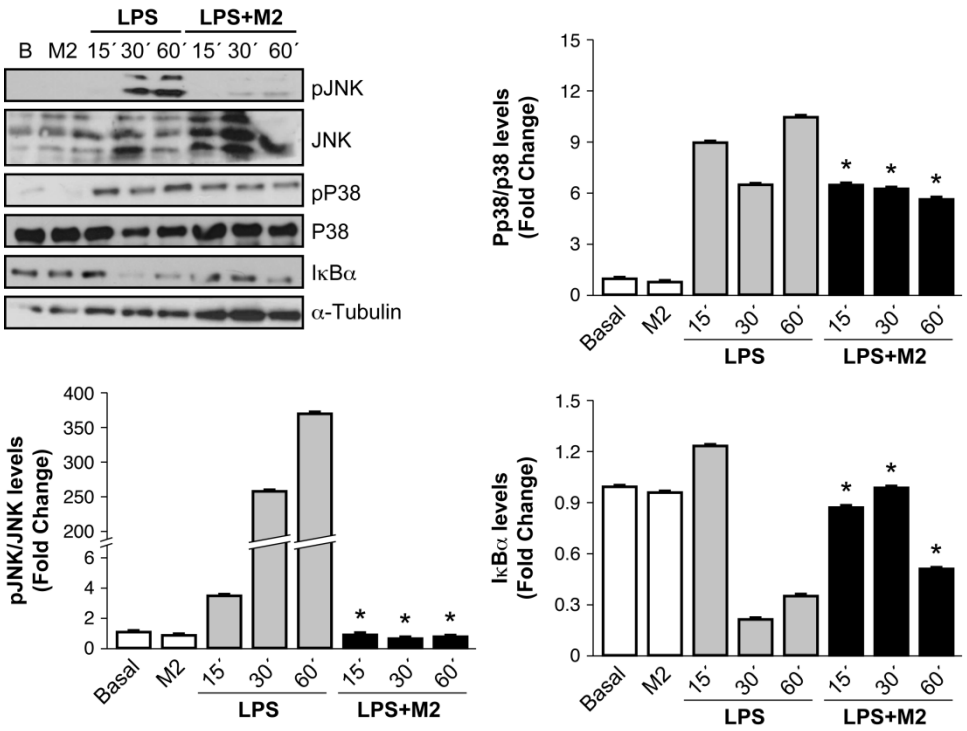

Figure 4. M2 cytokines decreased the pro-inflammatory signaling pathways induced by LPS in Bv-2 cells. Bv-2 cells were treated with LPS (200 ng/ml) in the absence or presence of IL4/IL13 (20 ng/ml each) for the indicated time-periods. Protein extracts (30 µg) were separated by SDS-PAGE and analyzed by Western blot with antibodies against phospho-JNK, total JNK, phospho-p38 MAPK, total p38 MAPK and IκBα. α-tubulin was used as a loading control. Representative autoradiograms are shown (n=6 independent experiments). The blots were quantitated by scanning densitometry. The results are means ± SEM. Data were analyzed by one-way ANOVA followed by Bonferroni t-test; *p≤ 0.05 LPS+M2 *vs* LPS.

The effect of *R-DS-ONJ* on the early proinflammatory signaling pathway induced by LPS in Bv-2 cells was also analyzed. Co-treatment with *R-DS-ONJ* prevented LPS-mediated IκBα degradation, the phosphorylation of JNK and p38 MAPK (Figure 5A). As Figure 5B shows, the treatment with R-DS-ONJ in presence of LPS prevents from NFkB p65 translocation to the nucleus.

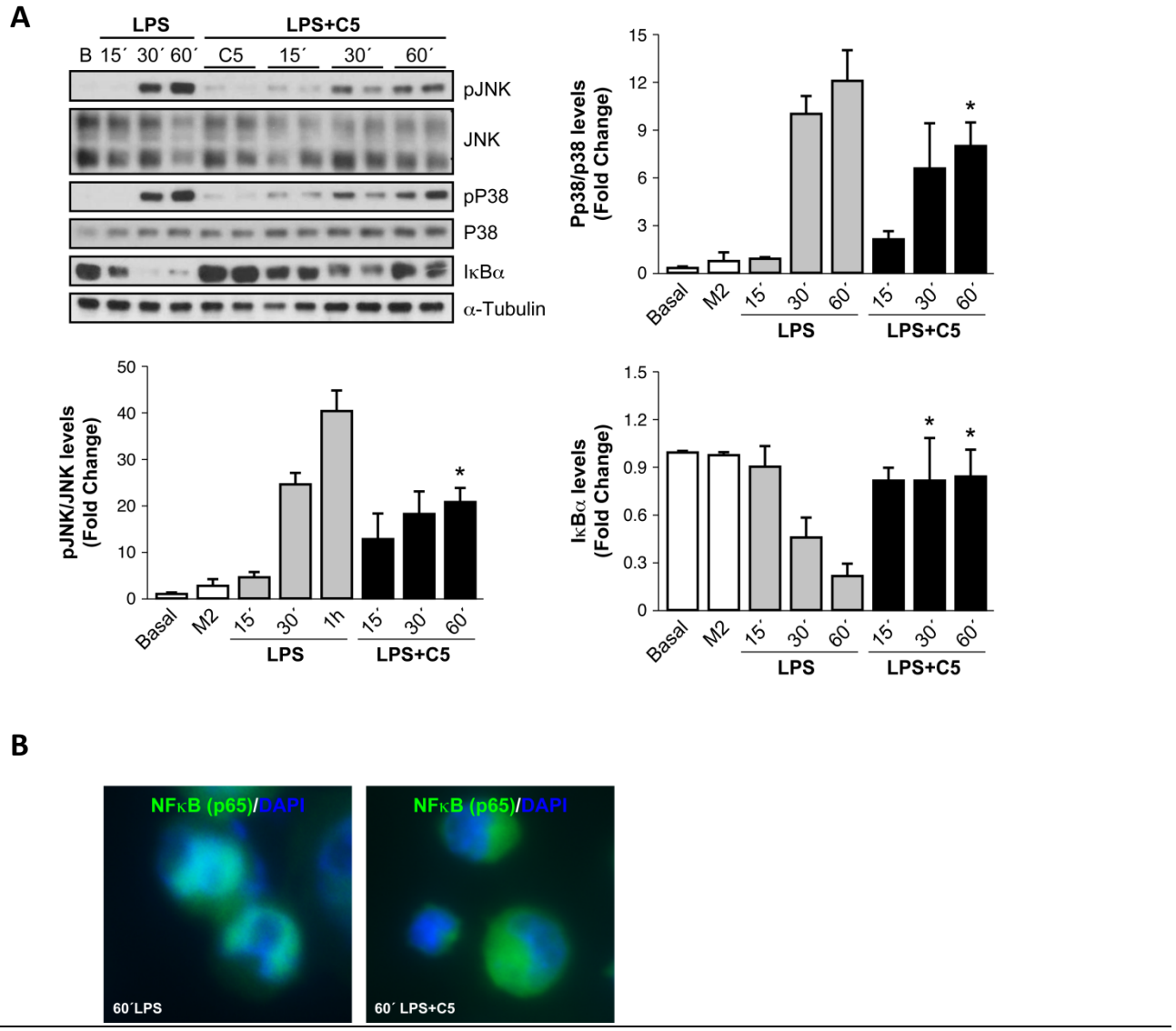

Figure 5. *R*-DS-ONJ decreased the pro-inflammatory signaling pathways induced by LPS in Bv-2 cells. Bv-2 cells were treated with LPS (200 ng/ml) in the absence or presence of *R*-DS-ONJ (50 μM) for the indicated time-periods. A) Protein extracts (30 μg) were separated by SDS-PAGE and analyzed by Western blot with antibodies against phospho-JNK, total JNK, phospho-p38 MAPK, total p38 MAPK and IκBα. α-Tubulin was used as a loading control. Representative autoradiograms are shown (n=6 independent experiments). The blots were quantities by scanning densitometry. The results are means ± SEM. Data were analyzed by one-way ANOVA followed by Bonferroni t-test; *p≤ 0.05 LPS+*R*-DS-ONJ *vs* LPS. B) Bv-2 cells treated for 60 min with LPS in the absence or presence of *R*-DS-ONJ were immunostained for p65 NFκB (green) and counterstained with DAPI (blue). Representative images are shown.

3.3. Sp²-iminosugar derived R-DS-ONJ prevented gliosis and M1 status associated to inflammation in retinas from db/db mice during DR

In order to determine the appropriate time-period in which to analyze the effect of Sp2-iminosugar derived R-DS-ONJ in retinal explants of *db/db* mice, we first study several parameters related to inflammation in circulation and in the retina in this mouse model.

During obesity, increased intestinal permeability leads to the leakage of bacterial products into the circulation that exacerbates the pro-inflammatory responses (27). Higher levels of serum endotoxin were detected in *db/db* mice at 5 weeks compared to age-matched *db/+* controls (Figure 6A) and these differences were maintained up to 20 weeks. Next, we evaluated the impact of the circulating endotoxemia on the inflammatory markers in the retina. Whereas in the retina of *db/db* mice iNOS mRNA and protein levels peaked at 5 weeks and remained elevated up to 8 weeks in comparison to age-matched *db/+* controls, arginase-1 mRNA and protein levels increased at 5-6 weeks and returned to basal levels at 8 weeks. These data reflect the decrease in the anti-inflammatory profile of the retina in *db/db* mice during DR progression (Figure 6B).

The immunofluorescence analysis in retinal sections revealed iNOS specific immunostaining (green) in OS (outer segment), OPL (outer plexiform layer), INL (inner nuclear layer) and GCL (ganglion cell layer) at 5 and 8 weeks in *db/db* mice, being immunolabelling stronger at 8

weeks (Figure 6C).

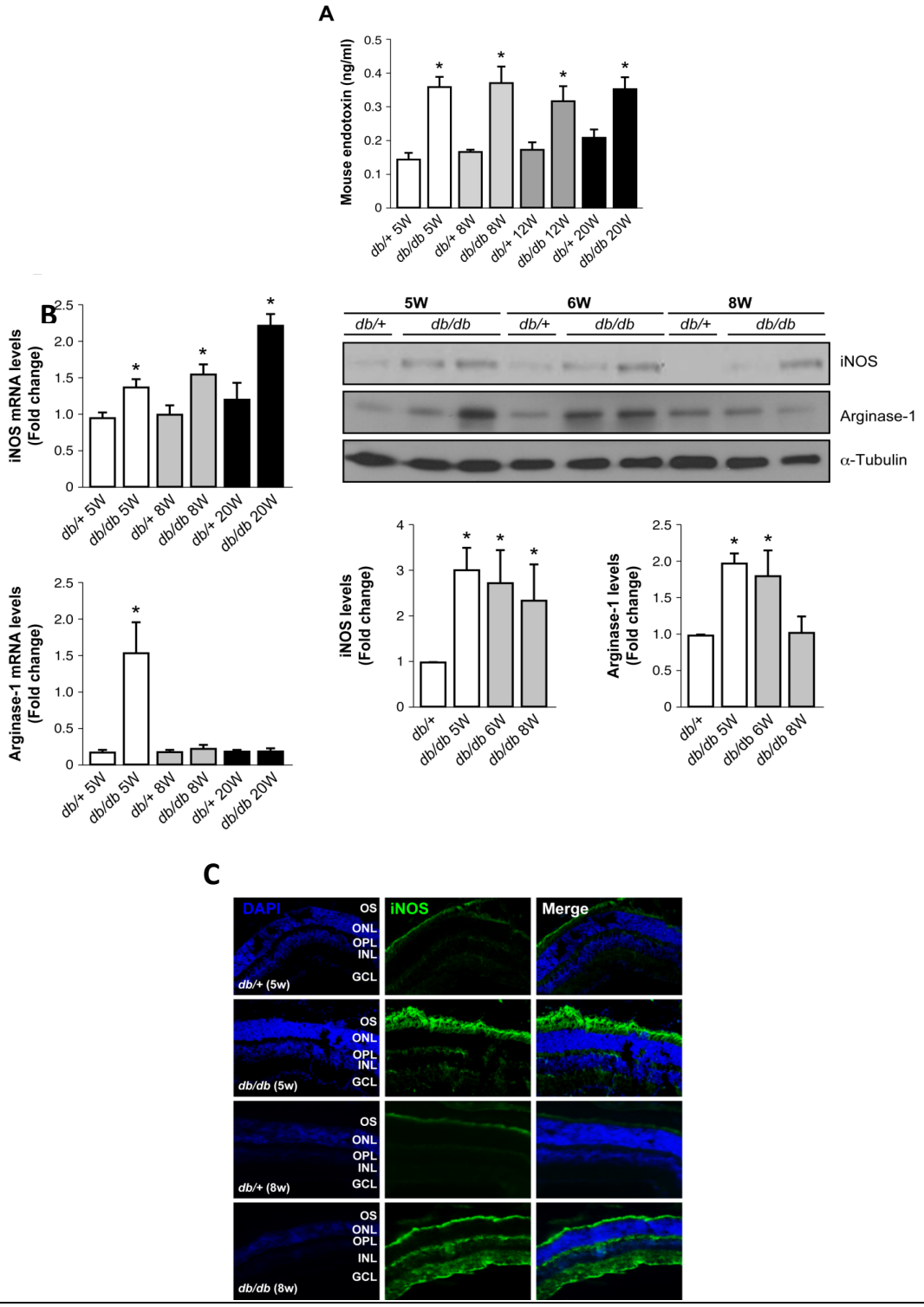

Figure 6. Circulating endotoxemia and pro-inflammatory cytokines during DR progression in *db/db* mice. A) Serum endotoxin in *db/db* and *db/+* mice at different ages. Results are means ± SEM (n=5 retinas per condition). *p≤0.05 *db/db* vs *db/+* matched at each age. B) (left panel) M1 (iNOS) and M2 (arginase-1) mRNAs in *db/db* and *db/+* mice at 5, 8 and 20 weeks. Results are expressed as $2^{-\Delta Ct}$. (right panel) iNOS and arginase-1 protein levels in retinas from *db/db* and *db/+* mice analyzed by Western blot at the ages indicated. Results are means ± SEM (n=5 retinas per condition). *p≤0.05 *db/db* vs *db/+* matched at each age. C) iNOS immunostaining (green) counterstained with DAPI (blue) (n=5 retinas per condition). Retinal layers are labelled as ONL (outer nuclear layer), OPL (outer plexiform layer), INL (inner nuclear layer), (IPL) inner plexiform layer and GCL (ganglion cell layer). At least 3 retinas and 4 non-adjacent sections per retina were analyzed for each experimental condition.

Based on these analysis of the inflammatory profile of the retina in *db/db* mice during DR progression, we performed the ex vivo analysis in retinal explants at 8 weeks of age. Retinal explants from 8 weeks old *db/+* and *db/db* mice treated for 24 h with *R*-DS-ONJ showed increased arginase-1 expression (M2 marker) compared to their respective untreated retinas (Figure 7A). Moreover, reactive gliosis, which was already present in retinas from *db/db* mice at 8 weeks (28) was maintained in retinal explants and decreased by the treatment with *R*-DS-ONJ (Figure 7B).

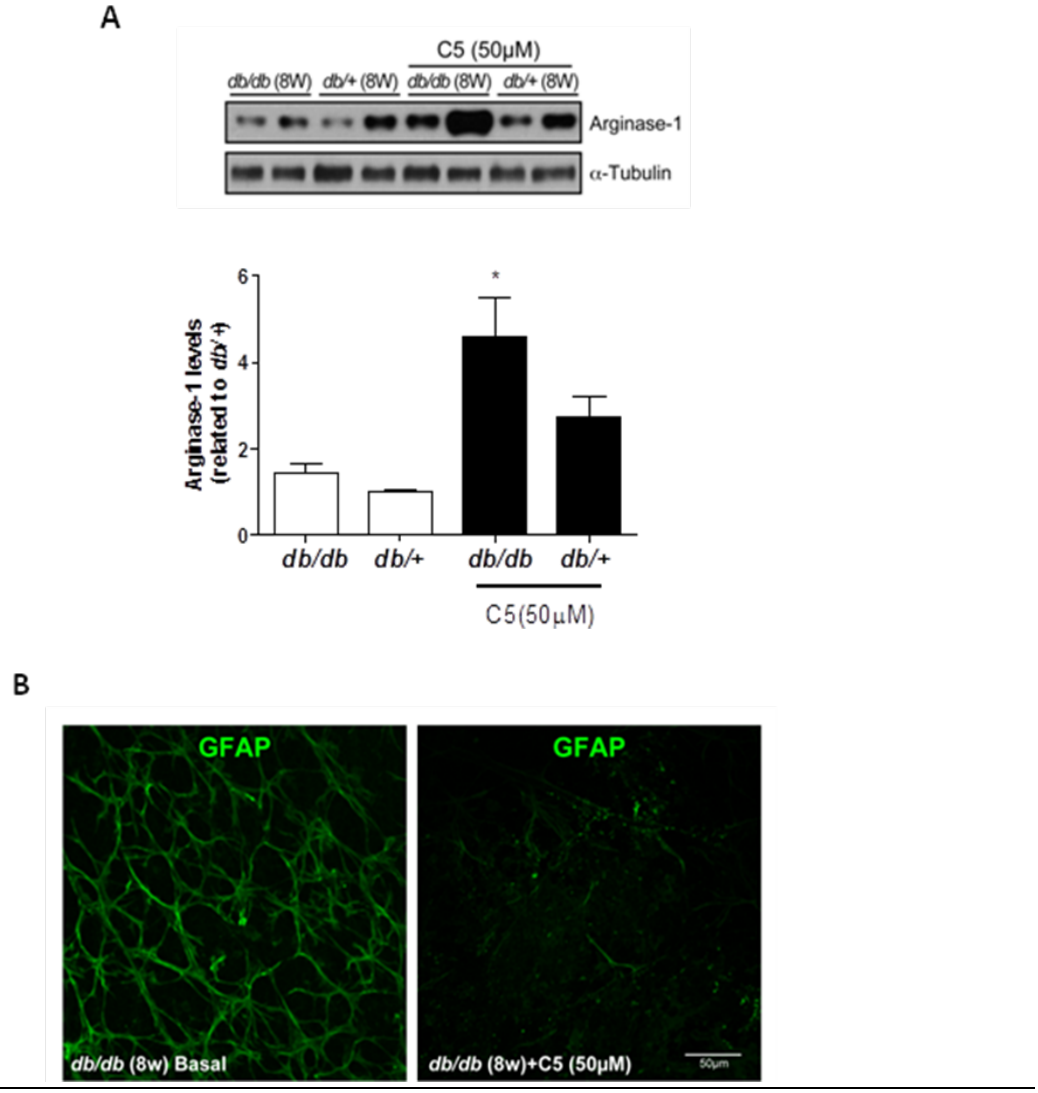

Figure 7. Retinal gliosis is detected in 8 weeks-old *db/db* mice. Retinal explants from 8 weeks old *db/+* and *db/db* mice were treated for 24 h with R-DS-ONJ. A) Western blot for arginase-1 (n=5 retinas per condition) G) Representative immunostaining for GFAP in whole retina.

4. DISCUSSION

T2D is considered a chronic low-grade systemic inflammatory disease characterized by changes in both the secretion of cytokines and the polarization of tissue-resident macrophages towards a M1 state (29-31) as demonstrated by the increased plasma levels of pro-inflammatory cytokines and C-reactive protein found in diabetic patients (32, 33). Among diabetic complications, DR is a multifactorial disease in which hyperglycaemia, inflammation and neuronal dysfunction are major factors involved in its etiopathology (34).

db/db mice recapitulate human DR progression and, therefore, these mice have been extensively used to study relevant processes such as retinal vascular leakage and neurodegeneration, as well to test potential pharmacological approaches (20, 35). Herein we have used for the first time *db/db* mice to characterize the microglia polarization during DR in a systemic pro-inflammatory environment. Notably, at 5 weeks of age, systemic endotoxemia was detected in *db/db* mice, probably reflecting alterations in intestinal barrier permeability and gut microbiota at this early period (36, 37). Although circulating TNFα and IL6 are elevated in 5 weeks old *db/db* mice (results not shown), the local inflammation in the retina was not manifested at this age since mRNA

levels of pro-inflammatory cytokines remained similar as in age-matched *db*+ lean mice. However, the analysis of M1/M2 markers in total retina revealed the coexistence of elevated iNOS (M1) and arginase-1 (M2) mRNA and protein levels only at an early stage of DR (5 weeks), both markers being localized mainly in the IPL, OPL and GCL where microglia was immunodetected. By contrast, in retinas of *db/db* mice at 8 weeks both the decrease in arginase-1 and the maintenance of high expression of iNOS paralleled the IL6 and TNFα mRNA levels. Taken together, these data indicate that in the retina of *db/db* mice the loss of the anti-inflammatory defense correlated with deterioration of the visual function in an age-dependent manner (20). Importantly, in retinas from *db/db* mice at 8 weeks treatment with R-DS-ONJ reduced GFAP immunostaining and also increased arginase-1, reflecting a regression towards an early stage of DR.

This study also provides new mechanistic insights in an in vitro bioassay that mimics the pro-inflammatory context of DR. We have used LPS as a pro-inflammatory stimulus in Bv-2 mouse microglia cell line since the M1 response of these cells resembles the in vivo situation in *db/db* mice in the course of DR. In Bv-2 microglial cells treated with LPS, the co-treatment with IL4/IL3 (M2 cytokines) or the sp^2-iminosugar dodecylsulfoxide *R*-DS-ONJ ameliorated the M1 phenotype induced by endotoxemia, as reflected by decreases in iNOS, nitrites and reduction of expression/secretion of pro-inflammatory cytokines. At the molecular level, treatment with M2 cytokines or *R*-DS-ONJ decreased the early activation of stress kinases (JNK and p38 MAPK) (38), prevented IκBα degradation and nuclear translocation of NF-κB.

5. CONCLUSION

Our results have shown for the first time the dynamics of microglia polarization during DR evolution in *db/db* mice and strongly suggest that targeting neuroinflammation by switching microglia towards a M2 polarization state might be a therapeutic strategy to delay and/or prevent the deterioration of visual function in diabetic patients.

6. ABBREVIATIONS

CNS: Central Nervous System

DR: Diabetic Retinopathy

FELASA: Federation of European Laboratory Animal Science Associations

GCL: Ganglion Cell Layer

GFAP: Glial Fibrillar Acidic Protein

IκBα: Nuclear Factor of kappa light polypeptide gene enhancer in B-cells Inhibitor, alpha

INL: Inner Nuclear Layer

JNK: c-Jun N-terminal kinase

LPS: Lipopolissacharide

mRNA: messenger Ribonucleic Acid

OPL: Outer Plexiform Layer

OS: Outer Segment

p38 MAPK: p38 Mitogen-activated Protein Kinase

qRT-PCR: quantitative Real-Time PCR

RNA: Ribonucleic Acid

RPE: Retinal Pigment Epithelium

SEM: Standar error of the Mean

7. CONFLICT OF INTEREST

The authors declare that there is no conflict of interest associated with this manuscript.

8. ACKNOWLEDGMENTS

We acknowledge Drs EM. Sánchez-Fernández, C. Ortiz Mellet and JM. García Fernández (University of Sevilla, Spain) for supplying C5. This work was supported by grants from the Spanish Ministry of Economy and Competitivity (SAF2015-65267-R and SAF2012-33283), Comunidad de Madrid S2010/BMD-2423 and S2010/BMD2439, Centro de Investigación Biomédica en Red de Diabetes y Enfermedades Metabólicas Asociadas (CIBERdem, Instituto Carlos III, Spain), European Union (EUROCONDOR (FP7 HEALTH.2011.2.4.3.1.)).

9. REFERENCES

1. Yau JW, Rogers SL, Kawasaki R, Lamoureux EL, Kowalski JW, Bek T, et al. Global prevalence and major risk factors of diabetic retinopathy. Diabetes care. 2012;35(3):556-64.
2. Simo R, Hernandez C. Novel approaches for treating diabetic retinopathy based on recent pathogenic evidence. Progress in retinal and eye research. 2015;48:160-80.
3. Tang J, Kern TS. Inflammation in diabetic retinopathy. Progress in retinal and eye research. 2011;30(5):343-58.
4. Abcouwer SF, Gardner TW. Diabetic retinopathy: loss of neuroretinal adaptation to the diabetic metabolic environment. Annals of the New York Academy of Sciences. 2014;1311:174-90.
5. Simo R, Hernandez C, European Consortium for the Early Treatment of Diabetic R. Neurodegeneration in the diabetic eye: new insights and therapeutic perspectives. Trends in endocrinology and metabolism: TEM. 2014;25(1):23-33.
6. Lynch JW. Native glycine receptor subtypes and their physiological roles. Neuropharmacology. 2009;56(1):303-9.
7. Zeng HY, Green WR, Tso MO. Microglial activation in human diabetic retinopathy. Archives of ophthalmology. 2008;126(2):227-32.
8. Krady JK, Basu A, Allen CM, Xu Y, LaNoue KF, Gardner TW, et al. Minocycline reduces proinflammatory cytokine expression, microglial activation, and caspase-3 activation in a rodent model of diabetic retinopathy. Diabetes. 2005;54(5):1559-65.
9. Mantovani A, Garlanda C. Platelet-macrophage partnership in innate immunity and inflammation. Nature immunology. 2013;14(8):768-70.

10. Mosser DM, Zhang X. Activation of murine macrophages. Current protocols in immunology / edited by John E Coligan [et al]. 2008;Chapter 14:Unit 14 2.
11. Martinez FO, Helming L, Gordon S. Alternative activation of macrophages: an immunologic functional perspective. Annual review of immunology. 2009;27:451-83.
12. Roquet A, Hallden G, Ihre E, Hed J, Zetterstrom O. Eosinophil activity markers in peripheral blood have high predictive value for bronchial hyperreactivity in patients with suspected mild asthma. Allergy. 1996;51(7):482-8.
13. Demircan N, Safran BG, Soylu M, Ozcan AA, Sizmaz S. Determination of vitreous interleukin-1 (IL-1) and tumour necrosis factor (TNF) levels in proliferative diabetic retinopathy. Eye. 2006;20(12):1366-9.
14. Hernandez C, Segura RM, Fonollosa A, Carrasco E, Francisco G, Simo R. Interleukin-8, monocyte chemoattractant protein-1 and IL-10 in the vitreous fluid of patients with proliferative diabetic retinopathy. Diabetic medicine : a journal of the British Diabetic Association. 2005;22(6):719-22.
15. Shi H, Zhang Z, Wang X, Li R, Hou W, Bi W, et al. Inhibition of autophagy induces IL-1beta release from ARPE-19 cells via ROS mediated NLRP3 inflammasome activation under high glucose stress. Biochemical and biophysical research communications. 2015;463(4):1071-6.
16. Butovsky O, Ziv Y, Schwartz A, Landa G, Talpalar AE, Pluchino S, et al. Microglia activated by IL-4 or IFN-gamma differentially induce neurogenesis and oligodendrogenesis from adult stem/progenitor cells. Molecular and cellular neurosciences. 2006;31(1):149-60.
17. Priestman DA, Platt FM, Dwek RA, Butters TD. Imino sugar therapy for type 1 Gaucher disease. Glycobiology. 2000;10(11):iv-vi.
18. Sanchez-Fernandez EM, Risquez-Cuadro R, Chasseraud M, Ahidouch A, Ortiz Mellet C, Ouadid-Ahidouch H, et al. Synthesis of N-, S-, and C-glycoside castanospermine analogues with selective neutral alpha-glucosidase inhibitory activity as antitumour agents. Chemical communications. 2010;46(29):5328-30.
19. Zhang L, Li R, Shi W, Liang X, Liu S, Ye Z, et al. NFAT2 inhibitor ameliorates diabetic nephropathy and podocyte injury in db/db mice. British journal of pharmacology. 2013;170(2):426-39.
20. Bogdanov P, Corraliza L, Villena JA, Carvalho AR, Garcia-Arumi J, Ramos D, et al. The db/db mouse: a useful model for the study of diabetic retinal neurodegeneration. PloS one. 2014;9(5):e97302.
21. Almeida JL, Hill CR, Cole KD. Mouse cell line authentication. Cytotechnology. 2014;66(1):133-47.
22. Arroba AI, Revuelta-Cervantes J, Menes L, Gonzalez-Rodriguez A, Pardo V, de la Villa P, et al. Loss of protein tyrosine phosphatase 1B increases IGF-I receptor tyrosine phosphorylation but does not rescue retinal defects in IRS2-deficient mice. Investigative ophthalmology & visual science. 2013;54(6):4215-25.
23. Badisa RB, Tzakou O, Couladis M, Pilarinou E. Cytotoxic activities of some Greek Labiatae herbs. Phytotherapy research : PTR. 2003;17(5):472-6.
24. Green LC, Wagner DA, Glogowski J, Skipper PL, Wishnok JS, Tannenbaum SR. Analysis of nitrate, nitrite, and [15N]nitrate in biological fluids. Analytical biochemistry. 1982;126(1):131-8.
25. Arroba AI, Alvarez-Lindo N, van Rooijen N, de la Rosa EJ. Microglia-mediated IGF-I neuroprotection in the rd10 mouse model of retinitis pigmentosa. Investigative ophthalmology & visual science. 2011;52(12):9124-30.
26. Boutagy NE, Neilson AP, Osterberg KL, Smithson AT, Englund TR, Davy BM, et al. Short-term high-fat diet increases postprandial trimethylamine-N-oxide in humans. Nutrition research. 2015;35(10):858-64.
27. Boutagy NE, McMillan RP, Frisard MI, Hulver MW. Metabolic endotoxemia with obesity: Is it real and is it relevant? Biochimie. 2016;124:11-20.
28. Arroba AI, Alcalde-Estevez E, Garcia-Ramirez M, Cazzoni D, de la Villa P, Sanchez-Fernandez EM, et al. Modulation of microglia polarization dynamics during diabetic retinopathy in db/db mice. Biochimica et biophysica acta. 2016;1862(9):1663-74.
29. Olefsky JM, Glass CK. Macrophages, inflammation, and insulin resistance. Annual review of physiology. 2010;72:219-46.
30. Hotamisligil GS. Inflammation and endoplasmic reticulum stress in obesity and diabetes. International journal of obesity. 2008;32 Suppl 7:S52-4.
31. Westcott DJ, Delproposto JB, Geletka LM, Wang T, Singer K, Saltiel AR, et al. MGL1 promotes adipose tissue inflammation and insulin resistance by regulating 7/4hi monocytes in obesity. The Journal of experimental medicine. 2009;206(13):3143-56.
32. Kahn SE, Hull RL, Utzschneider KM. Mechanisms linking obesity to insulin resistance and type 2 diabetes. Nature. 2006;444(7121):840-6.
33. Kim JK. Fat uses a TOLL-road to connect inflammation and diabetes. Cell metabolism. 2006;4(6):417-9.
34. Gardiner TA, Canning P, Tipping N, Archer DB, Stitt AW. Abnormal Glycogen Storage by Retinal Neurons in Diabetes. Investigative ophthalmology & visual science. 2015;56(13):8008-18.
35. Jung E, Kim J, Kim CS, Kim SH, Cho MH. Gemigliptin, a dipeptidyl peptidase-4 inhibitor, inhibits retinal pericyte injury in db/db mice and retinal neovascularization in mice with ischemic retinopathy. Biochimica et biophysica acta. 2015;1852(12):2618-29.

36. Brun P, Castagliuolo I, Di Leo V, Buda A, Pinzani M, Palu G, et al. Increased intestinal permeability in obese mice: new evidence in the pathogenesis of nonalcoholic steatohepatitis. American journal of physiology Gastrointestinal and liver physiology. 2007;292(2):G518-25.
37. Cani PD, Possemiers S, Van de Wiele T, Guiot Y, Everard A, Rottier O, et al. Changes in gut microbiota control inflammation in obese mice through a mechanism involving GLP-2-driven improvement of gut permeability. Gut. 2009;58(8):1091-103.
38. Traves PG, Pimentel-Santillana M, Rico D, Rodriguez N, Miethke T, Castrillo A, et al. Anti-inflammatory actions of acanthoic acid-related diterpenes involve activation of the PI3K p110gamma/delta subunits and inhibition of NF-kappaB. Chemistry & biology. 2014;21(8):955-66.